Forming Active Carbon Monoliths from H_3PO_4-loaded Sawdust with Addition of Peanut Shell Char

Dawei Li,[a,b] Yuanyu Tian,[a,b,*] and Yingyun Qiao [b]

Peanut shell char (PSC) was converted into active carbon monoliths (ACMs) by adding a binder that was easy to make. The conversion process involved adding the PSC into H_3PO_4-loaded sawdust, extruding the mixture, and finally heating the resulting monoliths for different times. The properties of the resulting ACMs were investigated using scanning electron microscopy, energy dispersive X-ray spectroscopy, Fourier transform infrared analysis, nitrogen adsorption-desorption, X-ray diffraction, and thermogravimetric analysis. The H_3PO_4-loaded sawdust could be used as a binder for converting powdered PSC into well-shaped ACMs without visual cracks. The resulting ACMs maintained their monolithic shape, even in water. The ACMs showed a much higher specific surface area (SSA, 850 to 915 m^2/g) than the PSC (105 m^2/g). The largest SSA (915 m^2/g) was achieved by activation for 50 min. Increasing the activation time decreased the SSA and apparent density, but only slightly impacted the carbon structure. This research might lead to value-added conversion of bio-chars.

Keywords: Peanut shell; Bio-char; Active carbon monolith; Sawdust; Phosphoric acid; Activation

Contact information: a: State Key Laboratory of Heavy Oil Processing, China University of Petroleum (East China), Qingdao, 266555, China; b: Research Centre for Low-carbon Energy Sources, Shandong University of Science and Technology, Qingdao, 266590, China;
**Corresponding author: shuxuewuli@126.com*

INTRODUCTION

Pyrolysis of biomass for bio-oils is considered to be an important strategy for remedying problems related to the depletion of fossil fuels and environmental pollution because bio-oils are promising candidates for the production of energy and value-added chemicals (Lu *et al.* 2008). The pyrolysis processes always yield solid byproducts, namely bio-chars, which usually account for about 10 wt% to 40 wt% of the biomass (Peng *et al.* 2012). The accumulation of the bio-chars can induce problems like space consumption, fire hazards, and environmental pollution. Hence, there is a need to convert the bio-chars into useful materials.

Given the abundance of carbon in bio-chars, the chars can be used as precursors for producing active carbons. To date, active carbons have been successfully prepared from bio-chars by physical or chemical activation (De *et al.* 2013; Gonzalez *et al.* 2009; Ismadji *et al.* 2005). However, most of the yielded active carbons are in the form of powders or small granules with particle sizes of less than 2 mm. Such active carbons are likely difficult to transport, process, and recycle due to innate drawbacks like low density, inferior volumetric adsorption capacity, and small mechanical strength (Xia and Mokaya 2007). To overcome these shortcomings, it is necessary to convert bio-chars into monolithic active carbons. However, the conversion of powdered bio-chars into active carbon monoliths (ACMs) has rarely been reported.

Active carbon monoliths (ACMs) are needed in applications such as gas adsorption, wastewater treatment, and energy storage because of their high density, superior volumetric adsorption capacity, and large mechanical strength (Xia and Mokaya 2007). A commonly used method for preparing ACMs with large SSAs involves extruding powdered active carbon along with organic matter-based binders such as coal tar pitch (Alcaniz-Monge *et al.* 2012), phenol resin (Machnikowski *et al.* 2012), polyvinyl alcohol (Balathanigaimani *et al.* 2009), carboxymethyl cellulose sodium salt (Balathanigaimani *et al.* 2009), and coal tar-methylcellulose-bean oil mixture (Liu *et al.* 2007). Nevertheless, most of these binders are difficult to obtain because their preparation processes are complicated or their precursors are derived from non-renewable resources. Hence, it is necessary to explore binders that are easily made.

In our previous research (Li *et al.* 2014), waste sawdust was successfully converted into binderless active carbon monoliths by activation with H_3PO_4. This result suggests that H_3PO_4-loaded sawdust could be used as a simple binder for converting bio-chars into ACMs. Additionally, in China, more than 4.5 Mt of peanut shell is generated annually, with most of them discarded or burnt. Pyrolysis of peanut shell for bio-oils is considered a promising technology for utilization of the waste biomass. However, the process generates plenty of peanut shell char (PSC) which needs disposing.

Given the necessity to change bio-chars into ACMs using easily-made binders, this research aimed to investigate the feasibility of converting a bio-char (PSC) into ACMs by adding H_3PO_4-loaded waste sawdust. The morphologies, textural properties, surface chemistry, microcrystalline structures, thermal stabilities, and yields of the ACMs produced at different activation times were investigated. This research might lead to high-value added utilization of bio-chars.

EXPERIMENTAL

Materials

Peanut shell char was produced by carbonizing air-dried peanut shell in a tube furnace (inner diameter: 70 mm) at 520 °C for 20 min. Waste Korean aspen (*Populus davidiana*) sawdust was provided by China Qingdao Jiaonanlongquan Wood Processing Co. Ltd. The particle size, volatile matter, fixed carbon, and ash content for the dried sawdust were 0.2 to 0.9 mm, 81.3%, 17.1%, and 1.6%, respectively, whereas the corresponding values for the dried peanut shell char (PSC) were < 0.074 mm, 4.0%, 90.8%, and 5.2%, respectively. The volatile matter was estimated by heating under N_2 at 670 °C for 3 h. The ash was determined by ashing in air at 670 °C for 3 h. The fixed carbon was calculated from the ash and the volatile matter. Phosphoric acid (AR) was supplied by China Yantai-Shuangshuang Co. Ltd.

Methods

Preparation of active carbon monoliths

The H_3PO_4-loaded waste aspen sawdust was prepared by mixing the sawdust with a 60 wt% H_3PO_4 solution at a H_3PO_4/sawdust mass ratio of 1.7:1. Subsequently, the H_3PO_4-loaded sawdust was added to the peanut shell char (PSC) at a dry-basis sawdust/ PSC mass ratio of 1:0.4. Then, the yielded mixture was stirred for 5 min and oven-heated at 85 °C for 1 h with intermittent stirring. Afterwards, the heated mixture (3.00 g) was converted into a monolith by pressing in a 2.0-cm inner-diameter cylindrical mould at 5 MPa. The yielded

monolith was then moved under N_2 to the heating zone of a tube furnace that had reached 560 °C. After heating for 50 min, 100 min, or 160 min, the heated monolith was cooled to room temperature, washed with hot deionized water until the eluate pH was about neutral, and finally dried first at 50 °C overnight and then at 105 °C for 2 h to produce an ACM. For the preparation of ACMs, the activation temperature was fixed at 560 °C because our preliminary experiments showed that the ACMs were liable to be visually crack-free under these conditions (Li *et al.* 2014). Hence, only the activation time was varied. The resulting ACMs were named ACMy, where y represents the activation time. For instance, ACM50 denotes an ACM made by activation at 560 °C for 50 min, with the other process parameters as mentioned above.

Preparation of active carbons from sawdust and peanut shell char

To investigate the reason for formation of pores in the ACMs, active carbons were also prepared from the PSC and the sawdust independently. The preparation process was the same as the one for the preparation of the ACMs (*e.g.*, heat treatment temperature) except that (1) the mass ratio of pure H_3PO_4 to the PSC (or the sawdust) was maintained at 1.7:1.4, and (2) the activation time was fixed at 100 min. The yielded active carbons were recorded as PSC100 and SD100, which represent active carbons prepared from the PSC and sawdust by activation at 560 °C for 100 min, respectively.

Analytical methods

Nitrogen adsorption/desorption isotherms were measured by an automatic surface area and pore analyzer (Tristar II 3020, Micromeritics Corp., USA) at 77 K. The micropore volume (V_{micro}) was determined using the t-plot method. The total pore volume (V_t) was estimated to be the liquid volume of N_2 adsorbed at a relative pressure of 0.95. The mesopore volume (V_{meso}) was calculated by subtracting the V_{micro} from the V_t . The micropore fraction (V_{micro}/V_t) was obtained by dividing the V_{micro} with the V_t. The apparent specific surface area (S_{BET}, SSA) was determined using the BET equation. The reported S_{BET} and V_t were both average of two replicates. The pore size distribution curves were obtained by applying the Barrett-Joyner-Halenda method to the desorption isotherms.

X-ray diffraction (XRD) patterns of the ACMs were acquired on an X-ray diffractometer (Max2500PC, MacScience Corp.; Japan) using an acceleration voltage of 30 kV and a current of 100 mA.

The apparent density of each ACM was recorded as its mass/volume ratio. The volume was calculated from the height and the top-surface diameter of the ACM. The reported apparent density is the average of two replicates.

The yield of porous carbon (active carbon or ACM) was recorded as the dry-basis weight ratio of the porous carbon to its precursors (sawdust for SD100, peanut shell for PSC100, and sawdust plus peanut shell for the ACMs).

The weight loss on washing (*WLW*) was used to estimate the amount of phosphorus-containing species removed from each 560 °C-heated monolith by the washing step. Each sample was washed seven times. For each time, the sample was shaken with 150 mL of water at 45 °C at 200 rpm for 50 min. The *WLW* was calculated as $WLW=1-W_a/W_b$, where W_b and W_a are the dry-basis weights of each monolith before (W_b) and after washing (W_a), respectively. The reported *WLW* is the average of two replicates.

For clear visibility of the surface morphology of ACMs, the carbon samples were coated with gold before their surface morphologies were observed using a scanning electron microscope (SEM, S-4800, HITACHI Corp., Japan) at an acceleration voltage of

5.0 kV. An energy dispersive X-ray spectrometer (EDX, GENESIS XM2 SYSTEM 60x) coupled with the SEM was used to estimate the chemical composition.

The Fourier transform infrared (FTIR) transmission spectra were acquired on a Nicolet 6700 FTIR instrument (Nexus, USA) in a wave number range of 400 to 4000 cm^{-1} with a KBr pellet method. Before acquiring the spectra, the mixture of a carbon sample and KBr was mixed at a mass ratio of about 1/100, ground, and then pressed to a pellet.

The dry-basis ash contents for samples were determined by ashing at 670 °C for 3 h in a muffle furnace.

The thermal analyses of the ACMs were conducted using a thermogravimetric analyzer (TGA-Q500, TA Instruments, USA) by heating the sample (~10 mg) under N_2 (50 mL/min) from room temperature to 670 °C at 10 °C /min.

RESULTS AND DISCUSSION

Yield

The yields of the ACMs were around 36.0% (Table 1). The typical yield range was 20% to 45% for the active carbons prepared from various biomasses by activation with H_3PO_4 or $(NH_4)_2HPO_4$ (Kennedy *et al.* 2004; Timur *et al.* 2006; Rosas *et al.* 2008; Gao *et al.* 2011; Sun and Webley 2011). Hence, despite different precursors and preparation conditions, it is plausible that the yields of the ACMs agreed well with the values reported for the other biomass-based active carbons.

Table 1. Yield, Textural Properties, Apparent Density, and Ash Content of Peanut Shell Char and Porous Carbons

Samples	Yield (%)	S_{BET} (m^2/g)	V_t (mL/g)	V_{micro} (mL/g)	V_{meso} (mL/g)	V_{micro}/V_t (%)	Apparent density (mL/g)	Ash (%)
ACM50	35.0	915±8	0.70±0.01	0.54	0.16	77.1	0.435±0.008	5.8
ACM100	35.9	883±9	0.67±0.03	0.52	0.15	77.6	0.446±0.007	6.6
ACM160	36.6	850±11	0.63±0.02	0.51	0.12	81.0	0.478±0.007	7.5
SD100	_	1272±8	0.71±0.02	0.67	0.04	94.4	_	_
PSC100	_	176±12	0.08±0.02	0.07	0.01	87.5	_	_
PSC	_	105±10	0.05±0.03	0.04	0.01	20.0	_	5.2

Photos of ACMs

A photograph of active carbon monoliths (ACMs) is provided in Fig. 1. The ACMs were about 2 cm in diameter and 4 mm in thickness. They were all disk-shaped and visually crack-free, indicating that the powdered PSC was successfully converted into monoliths. To estimate the ability of the ACMs to maintain their monolithic structure in water, the yielded ACMs were separately placed in a 250-mL conical bottle containing 150 mL of distilled water at 30 °C. The bottles were then shaken at 295 rpm for 30 min. The weight of carbon powder separated from each monolith was found to be lower than 0.5 wt% of the ACM (on dry basis). These results showed that the ACMs kept their monolithic shape well, even in water.

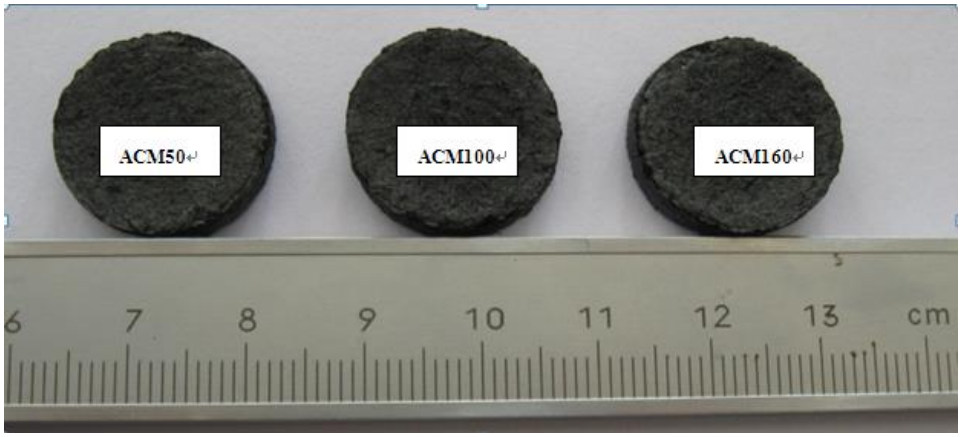

Fig. 1. Photograph of active carbon monoliths

Although the powdered PSC could be successfully converted into monoliths by adding H_3PO_4-loaded sawdust into the PSC, no monoliths were obtained when the sawdust or H_3PO_4 was independently added to the PSC. These facts indicated that the successful conversion of the powdered PSC into monoliths was attributable to the binding materials produced by the interaction between the sawdust and H_3PO_4. As a Brönsted acid and dehydrating agent, H_3PO_4 can depolymerize biopolymers (lignin, hemicellulose, *etc.*) of lignocellulosic precursors into smaller units (Jagtoyen and Derbyshire 1998; Nakagawa *et al.* 2007). The units have a high degree of mobility and can be converted into tars surrounding the char. The presence of tar was suggested by the observation that the H_3PO_4-loaded sawdust with a H_3PO_4/sawdust mass ratio of 1.7 turned into black sticky matter after heating at 85 °C for 1.5 h. The tar can make the precursors extrudable by acting as binders, and after carbonization, they can provide mechanical rigidity to the monoliths (Li *et al.* 2014; Rosas *et al.* 2008; Vargas *et al.* 2011). This may explain the formation of monoliths and their ability to maintain the monolithic shape in water. The important role of tar in monolith formation was also revealed by the fact that biomass could be converted into ACMs without using binders (Djeridi *et al.* 2013; Nakagawa *et al.* 2007; Vargas *et al.* 2011). Additionally, the ash contents of the ACMs were found to be low (5.8% to 7.5%, Table 1), suggesting that the inorganic residues in the samples were in small quantities. Hence, the binding roles of the inorganic matters in the ACMs should not be the main reason for the successful conversion of the PSC into monoliths.

Few studies have aimed to shape powdered bio-chars into active carbon monoliths (ACMs). Monolithic active carbons are expected to be more desirable for use, as they are much easier to transport, process, and recycle than the active carbons in the form of powders or small granules. Hence, the conversion of PSC into ACMs could likely increase the additional value of the bio-chars and solve bio-char-induced problems such as space consumption.

Also, it should be noted that the conversion of PSC into ACMs was achieved by adding H_3PO_4-loaded sawdust. Compared with commonly used binders like phenolic resin and coal tar pitch, the H_3PO_4-loaded waste sawdust was easy to make, as it could be readily prepared by impregnating an abundantly available waste biomass with H_3PO_4. Hence, it was concluded that the H_3PO_4-loaded sawdust is an easily-made binder that is applicable to the conversion of bio-chars into ACMs.

SEM Images and EDX Analysis

Figure 2 shows SEM images of PSC, ACM100, SD100, and PSC100. The PSC exhibited a dense, board-like structure with few macropores. In contrast, ACM100 was highly porous, having numerous tube-like macropores with sizes of 3 to 12 μm. The presence of large macropores could promote the rapid transport of species such as molecules and ions (Alvarez *et al.* 2004). Similar tube-like macropores were observed for H_3PO_4-activated sawdust (SD100), but not for H_3PO_4-activated peanut shell char (PSC100), indicating that the observed macropores for ACM100 were related to the H_3PO_4-activated sawdust (SD100). The formation of the macropores in the H_3PO_4-activated sawdust was attributable to the evaporation of sawdust constituents, decomposition of the activating agent, chemical reaction between the sawdust and the activator during activation, or the space previously occupied by the activator (Tang *et al.* 2012).

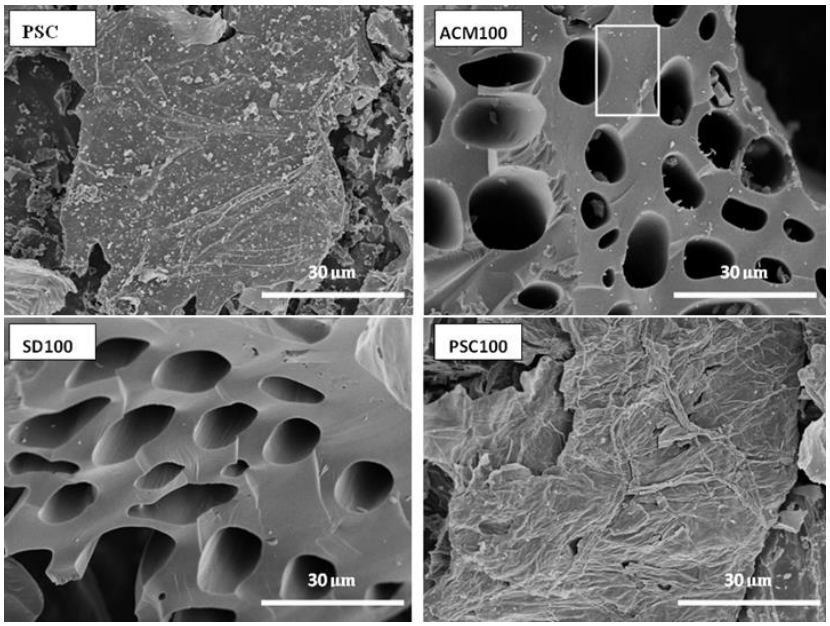

Fig. 2. SEM images of peanut shell char (PSC), active carbon monolith (ACM100), H_3PO_4-activated sawdust (SD100), and H_3PO_4-activated PSC (PSC100). The white rectangle on the image of ACM100 was the area used for EDX analysis

The relative contents of C, O, P, and Si for ACM100 were 82.4 wt%, 12.9 wt%, 3.6 wt%, and 1.1 wt%, respectively, as determined by EDX. The data indicated that phosphorus was not completely washed off the carbon materials under the washing conditions. This result agreed well with the incorporation of P into organic molecular structures, as indicated by the FTIR spectra (Fig. 3, to be discussed later). However, the amount of P was small.

FTIR Spectra

The FTIR spectra for the PSC, ACM50, and ACM160 are provided in Fig. 3. The bands around 3426 cm^{-1} and 1580 cm^{-1} were attributed to the O-H stretching in hydroxyl groups (Yang and Lua 2003) and C=C stretching vibration (Guo and Rockstraw 2007), respectively. The band at about 1370 cm^{-1} was assigned to the symmetrical bending of the C–H bond in the methyl group, while the bands at 864 cm^{-1}, 795 cm^{-1}, and 739 cm^{-1} were attributed to aromatic C–H out-of-plane bending vibrations (Yang and Lua 2003).

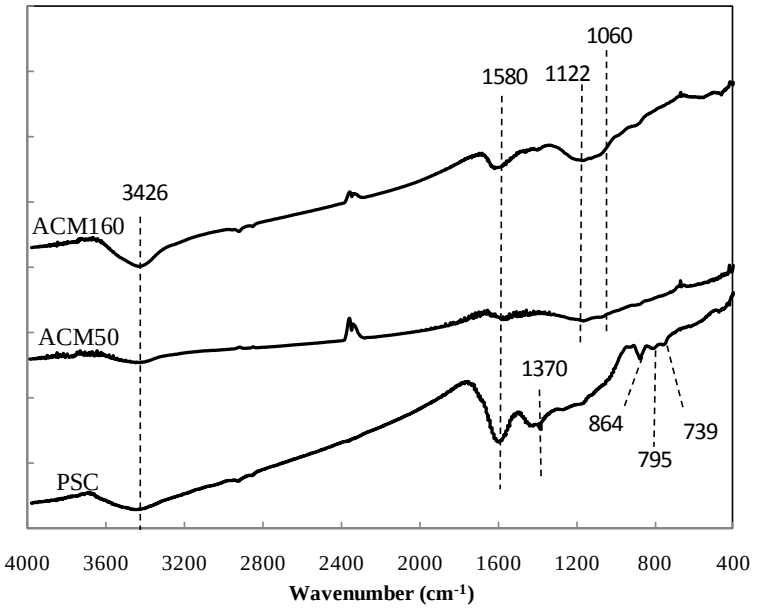

Fig. 3. FTIR spectra for peanut shell char (PSC) and active carbon monoliths (ACM50 & ACM160)

Compared with the bands for the C-H bonds of PSC, those of ACMs were hardly discernable, indicating that the hydrogen was removed. This removal was probably due to the heat treatment and the dehydrating effects of H_3PO_4. The broad band near 1060 cm^{-1} and a broad band shouldered at 1122 cm^{-1} indicated the presence of phosphorus-containing species in the ACMs (Kennedy *et al.* 2004), which coincided with the presence of phosphorus shown by the EDX results. The band at 1122 cm^{-1} can be assigned to the stretching of hydrogen-bonded P=O, to the O-C stretching vibrations in a P-O-C (aromatic) linkage, and to the P=OOH (Kennedy *et al.* 2004). The shoulder at 1060 cm^{-1} can be ascribed to the ionized linkage P^+-O^- in acid phosphate esters and the symmetrical vibration in a chain of P-O-P (polyphosphate) (Kennedy *et al.* 2004). The characteristic bands for the phosphorus-containing species of ACM160 were more intensive than those of ACM50, suggesting that as the activation time increased, more phosphorus-containing specs were retained in the ACMs. It has been reported that the presence of phosphorus on the activated carbon monoliths can promote the adsorption of water vapor (Rosas *et al.* 2008). Hence, the obtained ACMs might be used as desiccants.

XRD Analysis

The XRD patterns of the ACMs are provided in Fig. 4. The broad peaks located at around 23° and 43° are reflections from the (002) and (100) planes of microcrystals in the turbostratic graphite structure, respectively (Tang *et al.* 2012). The presence of the two peaks showed that the carbon structure of the ACMs was amorphous (Tang *et al.* 2012).

The peaks for the (002) planes were almost the same for the three ACMs, although their activation times were different. Similar results were found for the (100) planes. These results indicated that the carbon structure of the ACMs only changed slightly when the activation time increased.

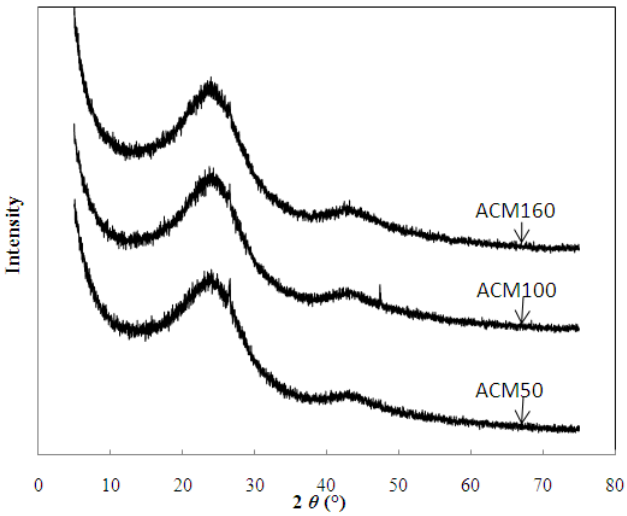

Fig. 4. XRD patterns for active carbon monoliths

TG Analysis

The thermogravimetric (TG) curves for the ACMs are presented in Fig. 5. The ACMs exhibited weight losses below 140 °C and above 540 °C, which were attributable to the release of adsorbed water/gas and to the thermochemical decomposition of fixed carbon, respectively. However, at temperatures between 140 and 540 °C, the weight was almost constant, indicating that the ACMs were stable in this temperature range.

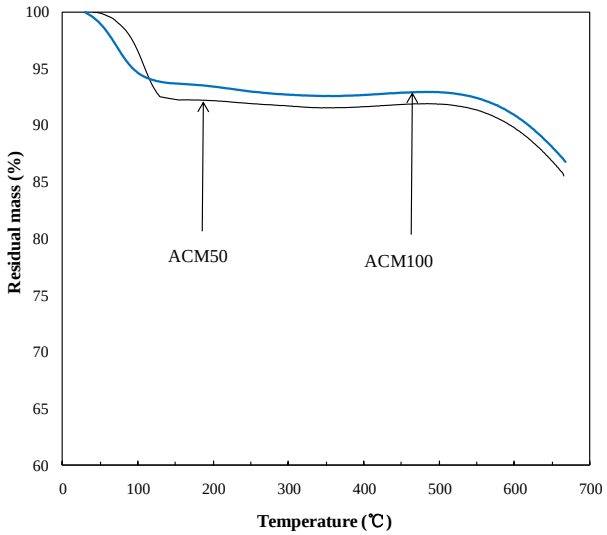

Fig. 5. Thermogravimetric analysis for two ACMs

Textural Properties

The adsorption-desorption isotherms of the ACMs are presented in Fig. 6a. The isotherms sharply increased at low pressures and exhibited hysteresis loops at relative pressures of 0.4 to 0.8. According to the IUPAC classification, the isotherms were a combination of type I and IV, indicating the presence of both micropores and mesopores. The micropore fractions were around 80.0% (Table 1). The high micropore fractions indicated the high potential of the ACMs in removing small molecules from polluted air or

waste water. The mesopores might be ink bottle-shaped, as the hysteresis loops were of type H2. The diameters of the mesopores were mostly in the range of 2 to 5 nm (Fig. 6b).

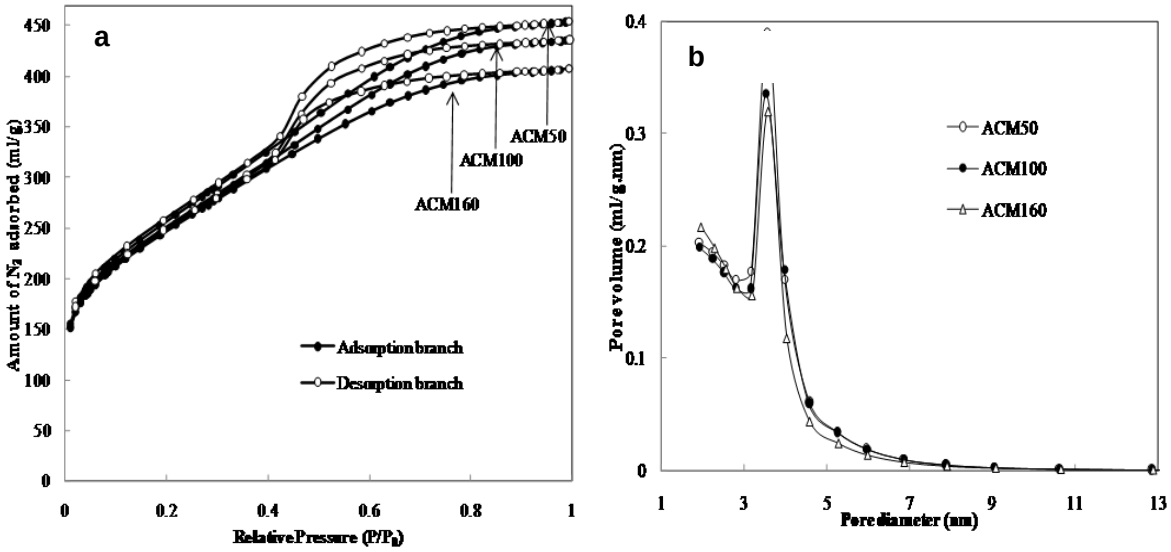

Fig. 6. (a) N_2 adsorption/desorption isotherms and (b) pore size distributions for active carbon monoliths

The textural properties of the ACMs are presented in Table 1. The SSAs of the ACMs were in the range of 850 to 915 m^2/g, which were comparable with the SSAs of ACMs prepared from olive stones (532 to 1014 m^2/g), rubber wood sawdust (534 to 913 m^2/g), and *Pinus sylvestris* (483 to 1152 m^2/g) (Li *et al.* 2014). The high SSAs indicated that the samples contained many pores and were highly porous. The high SSAs of the ACMs were assumed to result from the activation effects of H_3PO_4 on the PSC or the sawdust. To investigate the activation effects of H_3PO_4 on the PSC, the textural properties of PSC and PSC100 were determined (Table 1). The SSA of the H_3PO_4-activated PSC (PSC100) was only a little larger than that of PSC (176 m^2/g > 105 m^2/g), indicating that the activation effect of H_3PO_4 on the PSC under the preparation conditions was small. Hence, this effect should not be the main reason for the formation of the large SSAs of the ACMs.

To investigate the activation effects of H_3PO_4 on the sawdust, the SSA of the H_3PO_4-activated sawdust (SD100) and ACM100 were measured (Table 1). The SSA of the SD100 was much larger than that of ACM100 (1272 m^2/g > 883 m^2/g), suggesting that the H_3PO_4 had considerable activation effects on the sawdust. Similar activation effects were found for the preparation of active carbons from other biomass by activation with H_3PO_4 (Laszlo *et al.* 2005; Rosas *et al.* 2008). Hence, the formation of the SSAs of the ACMs should be primarily due to the activation effect of H_3PO_4 on the sawdust used to prepare the ACMs. This activation effect may be attributable to the role of washing, which removed phosphorus-containing species and thus yielded a carbon matrix with an accessible pore structure (Jagtoyen and Derbyshire 1998; Nakagawa *et al.* 2007; Rosas *et al.* 2008). The formation of phosphorus-containing species was a result of the fact that H_3PO_4 can degrade the biopolymers in the sawdust and can crosslink the biopolymer fragments to form phosphate and polyphosphate bridges (Jagtoyen and Derbyshire 1998; Nakagawa *et al.* 2007; Rosas *et al.* 2008). Additionally, the activation effects on the sawdust may be due to

the removal of volatile substances from the precursors, the removal being attributable to the thermopyrolysis and the reactions between H_3PO_4 (or its derived species) and the sawdust (Guo and Rockstraw 2007).

To sum up, the analysis of the SSAs showed that the large SSAs of the ACMs were primarily due to the activation effects of H_3PO_4 on the sawdust, rather than on the PSC.

In addition, Table 1 shows that when the activation time was prolonged, the SSA of ACMs decreased. This result was attributable to the increase in carbon skeleton contraction (Rosas *et al.* 2008; Sun and Webley 2011), which agreed well with the observation that the apparent density of ACM160 was larger than that of ACM50 (Table 1). Besides, the decrease in SSA with increasing activation time was likely a result of pore blockage. As the activation time increased, more phosphorus-containing species seemed to remain in the ACMs, which was revealed by the facts that (1) the FTIR bands for phosphorus-containing species were more intensive for the ACM prepared at longer activation times (Fig. 3), and (2) ACMs prepared at a prolonged activation time exhibited a lower weight loss on washing (56.7 ± 0.5%, 54.2 ± 0.3%, and 51.8 ± 0.3% for ACM50, ACM100, and ACM160, respectively). As a result, more pores would be blocked when the activation time was prolonged.

CONCLUSIONS

1. Peanut shell char could be converted into well-shaped ACMs without visual cracks by adding H_3PO_4-loaded sawdust. The H_3PO_4-loaded sawdust could be used as an easy-to-make binder for shaping powdered PSC into water-stable ACMs.
2. The resulting ACMs displayed large specific surface areas (850 to 915 m^2/g), with the largest SSA achieved by activation for 50 min.
3. The ACMs were amorphous carbons, with hydroxyl groups and phosphorus-containing groups present on their surfaces. Their yield was in the range of 35.0% to 36.6%.
4. Varying the activation time could change the SSA and apparent density, but could only slightly impact their microcrystalline structure.

ACKNOWLEDGEMENTS

We are grateful for the financial support provided by the National Natural Science Foundation of China (51206099), the Program for New Century Excellent Talent in University of the Ministry of Education of China (NCET-11-1031), and the National High Technology Research and Development Program of China (2012AA051801-2).

REFERENCES CITED

Alcaniz-Monge, J., Marco-Lozar, J. P., and Lozano-Castello, D. (2012). "Monolithic carbon molecular sieves from activated bituminous coal impregnated with a slurry of coal tar pitch," *Fuel Process. Technol*. 95(3), 67-72.

Alvarez, S., Esquena, J., Solans, C., and Fuertes, A. B. (2004). "Meso/macroporous carbon monoliths from polymeric foams," *Adv. Eng. Mater*. 6(11), 897-899.

Balathanigaimani, M. S., Shim, W.-G., Lee, J.-W., and Moon, H. (2009). "Adsorption of methane on novel corn grain-based carbon monoliths," *Micropor. Mesopor. Mater.* 119(1-3), 47-52.

De, M., Azargohar, R., Dalai, A. K., and Shewchuk, S. R. (2013). "Mercury removal by bio-char based modified activated carbons," *Fuel* 103(1), 570-578.

Djeridi, W., Ouederni, A., Wiersum, A. D., Llewellyn, P. L., and El Mir, L. (2013). "High pressure methane adsorption on microporous carbon monoliths prepared by olives-stones," *Mater. Lett.* 99(5), 184-187.

Gao, P., Liu, Z. H., Xue, G., Han, B., and Zhou, M. H. (2011). "Preparation and characterization of activated carbon produced from rice straw by $(NH_4)_2HPO_4$ activation," *Bioresour. Technol.* 102(3), 3645-3648.

Gonzalez, J. F., Roman, S., Encinar, J. M., and Martinez, G. (2009). "Pyrolysis of various biomass residues and char utilization for the production of activated carbons," *J. Anal. Appl. Pyrolysis* 85(1-2), 134-141.

Guo, Y., and Rockstraw, D. A. (2007). "Activated carbons prepared from rice hull by one-step phosphoric acid activation," *Micropor. Mesopor. Mater.* 100(1-3), 12-19.

Ismadji, S., Sudaryanto, Y., Hartono, S. B., Setiawan, L. E. K., and Ayucitra, A. (2005). "Activated carbon from char obtained from vacuum pyrolysis of teak sawdust: pore structure development and characterization," *Bioresour. Technol.* 96(12), 1364-1369.

Jagtoyen, M., and Derbyshire, F. (1998). "Activated carbons from yellow poplar and white oak by H_3PO_4 activation," *Carbon* 36(7), 1085-1097.

Kennedy, L. J., Vijaya, J. J., and Sekaran, G. (2004). "Effect of two-stage process on the preparation and characterization of porous carbon composite from rice husk by phosphoric acid activation," *Ind. Eng. Chem. Res.* 43(8), 1832-1838.

Laszlo, K., Onyestyak, G., Rochas, C., and Geissler, E. (2005). "Honeycomb carbon monoliths from *Pinus sylvestris*," *Carbon* 43(11), 2402-2405.

Li, D., Tang, R., Tian, Y., Qiao, Y., and Li, J. (2014). "Preparation of highly porous binderless active carbon monoliths from waste aspen sawdust," *BioResources* 9(1), 1246-1254.

Liu, L. S., Liu, Z. Y., Huang, Z. G., and Liu, Z. H. (2007). "Effect of coal rank on the properties of coal-based activated carbon honeycomb monoliths," *New Carbon Mater.* 22(1), 28-34.

Lu, Q., Yang, X. Y., and Zhu, X. F. (2008). "Analysis on chemical and physical properties of bio-oil pyrolyzed from rice husk," *J. Anal. Appl. Pyrolysis* 82(2), 191-198.

Machnikowski, J., Kierzek, K., and Torchala, K. (2012). "Adsorption capacity enhancement by activation with CO_2 of monolithic adsorbents made of KOH-activated carbon and polymer-derived binder," *Energy & Fuels* 26(6), 3697-3702.

Nakagawa, Y., Molina-Sabio, M., and Rodriguez-Reinoso, F. (2007). "Modification of the porous structure along the preparation of activated carbon monoliths with H_3PO_4 and $ZnCl_2$," *Micropor. Mesopor. Mater.* 103(1), 29-34.

Peng, F., He, P. W., Luo, Y., Lu, X., Liang, Y., and Fu, J. (2012). "Adsorption of phosphate by biomass char deriving from fast pyrolysis of biomass waste," *Clean-Soil Air Water* 40(5), 493-498.

Rosas, J. M., Bedia, J., Rodriguez-Mirasol, J., and Cordero, T. (2008). "Preparation of hemp-derived activated carbon monoliths: Adsorption of water vapor," *Ind. Eng. Chem. Res.* 47(4), 1288-1296.

Sun, Y., and Webley, P. A. (2011). "Preparation of activated carbons with large specific surface areas from biomass corncob and their adsorption equilibrium for methane, carbon dioxide, nitrogen, and hydrogen," *Ind. Eng. Chem. Res.* 50(15), 9286-9294.

Tang, Y. B., Liu, Q., and Chen, F. Y. (2012). "Preparation and characterization of activated carbon from waste *Ramulus mori*," *Chem. Eng. J.* 203(9), 19-24.

Timur, S., Kantarli, I. C., Ikizoglu, E., and Yanik, J. (2006). "Preparation of activated carbons from oreganum stalks by chemical activation," *Energy & Fuels* 20(6), 2636-2641.

Vargas, D. P., Giraldo, L., Silvestre-Albero, J., and Moreno-Pirajan, J. C. (2011). "CO_2 adsorption on binderless activated carbon monoliths," *Adsorption* 17(3), 497-504.

Xia, Y., and Mokaya, R. (2007). "Ordered mesoporous carbon monoliths: CVD nanocasting and hydrogen storage properties," *J. Phys. Chem. C* 111(27), 10035-10039.

Yang, T., and Lua, A. C. (2003). "Characteristics of activated carbons prepared from pistachio-nut shells by physical activation," *J. Colloid Interf. Sci*. 267(2), 408-417.

Article submitted: April 18, 2014; Peer review completed: June 7, 2014; Revised version received: June 20, 2014; Accepted: June 26, 2014; Published: July 8, 2014.